Journal of Controlled Release 208 (2015) 76–84

Contents lists available at ScienceDirect

Journal of Controlled Release

journal homepage: www.elsevier.com/locate/jconrel

A functionalized, injectable hydrogel for localized drug delivery with tunable thermosensitivity: Synthesis and characterization of physical and toxicological properties

Paul Z. Elias [a], Gary W. Liu [a], Hua Wei [a,1], Michael C. Jensen [c], Philip J. Horner [b,*], Suzie H. Pun [a,*]

[a] Department of Bioengineering and Molecular Engineering and Sciences Institute, University of Washington, Seattle, WA 98195, United States
[b] Department of Neurological Surgery, University of Washington, Seattle, WA 98195, United States
[c] Ben Towne Center for Childhood Cancer Research, Seattle Children's Research Institute, Seattle, WA 98101, United States

ARTICLE INFO

Article history:
Received 19 November 2014
Received in revised form 20 February 2015
Accepted 1 March 2015
Available online 4 March 2015

Keywords:
Injectable hydrogel
Peptide
Drug delivery
Cell therapy
Immunotherapy
Spinal cord injury

ABSTRACT

Thermosensitive injectable hydrogels have been used for the delivery of pharmacological and cellular therapies in a variety of soft tissue applications. A promising class of synthetic, injectable hydrogels based upon oligo(ethylene glycol) methacrylate (OEGMA) monomers has been previously reported, but these polymers lack reactive groups for covalent attachment of therapeutic molecules. In this work, thermosensitive, amine-reactive and amine-functionalized polymers were developed by incorporation of methacrylic acid N-hydroxysuccinimide ester or 2-aminoethyl methacrylate into OEGMA-based polymers. A model therapeutic peptide, bivalirudin, was conjugated to the amine-reactive hydrogel to investigate effects on the polymer thermosensitivity and gelation properties. The ability to tune the thermosensitivity of the polymer in order to compensate for peptide hydrophilicity and maintain gelation capability below physiological temperature was demonstrated. Cell encapsulation studies using an H9 T-cell line (CD4+) were conducted to evaluate feasibility of the hydrogel as a carrier for cellular therapies. Although this class of polymers is generally considered to be non-toxic, it was found that concentrations required for gelation were incompatible with cell survival. Investigation into the cause of cytotoxicity revealed that a hydrolysis byproduct, diethylene glycol monomethyl ether, is likely a contributing factor. While modifications to structure or composition will be required to enable viable cell encapsulation, the functionalized injectable hydrogel has the potential for controlled delivery of a wide range of drugs.

1. Introduction

Intraparenchymal, organ specific drug delivery is a challenge that could be met through development of engineered biomaterials. Thermosensitive injectable hydrogels are a promising class of biomaterials that are typically characterized by a lower critical solution temperature (LCST) above which they undergo a sol–gel transition. This property allows for injection in a liquid state and subsequent gelation after equilibration to physiological temperature in vivo [1,2]. Injectable hydrogels have utility in a variety of soft tissue applications where minimally invasive implantation and low stiffness can minimize damage to delicate anatomical structures.

Injuries and diseases of the central nervous system (CNS) are particularly difficult to access and challenging to treat, making them logical targets for advanced drug and cellular therapies delivered via hydrogel. One potential application of drug-loaded hydrogels is for treatment of spinal cord injury (SCI). Thermosensitive hydrogels are particularly attractive for spinal cord delivery since the blood–spinal cord barrier (BSCB) restricts the passage of most systemically-administered drugs into the spinal cord [3–5]. Local delivery of a therapeutic hydrogel formulation within spinal cord tissue therefore bypasses the BSCB and creates a local drug depot that increases delivery efficiency and organ specificity, while reducing drug exposure to potentially degradative enzymes in the circulation [4]. This is especially advantageous for delivery of peptide and protein therapeutics, which typically have short half lives in circulation and may be too large or hydrophilic to cross the BSCB. Further, peptides are amenable for covalent attachment to biomaterials since various functionalities for conjugation may be present or incorporated through particular amino acids. Therapeutic peptides have been identified that target various aspects of CNS pathophysiology following injury to the spinal cord, providing a range of potential drugs and associated targets [6]. Conjugation of one such peptide, bivalirudin, is demonstrated in this work. Bivalirudin is a 20 amino acid peptide which acts to directly inhibit thrombin and has been shown to provide beneficial effects in mitigating glial scarring after spinal cord injury [7].

* Corresponding authors.
E-mail addresses: phorner@uw.edu (P.J. Horner), spun@uw.edu (S.H. Pun).
[1] Current affiliation: Department of Chemistry, Lanzhou University, Lanzhou 730000, China.

http://dx.doi.org/10.1016/j.jconrel.2015.03.003
0168-3659/

Drug and cell-loaded hydrogels are also useful in oncology immunotherapies. In particular, injectable hydrogels could potentially be used following brain tumor resection to fill the resulting cavity and deliver drugs and/or anti-cancer T lymphocytes for targeting residual tumor cells [8]. For example, immunomodulatory peptides or proteins may be included in the hydrogel to enhance T-cell therapies [9]. However, cells must be able to survive and migrate within the hydrogel. This work therefore aims to develop an injectable hydrogel system potentially suitable for both controlled drug-delivery and cellular encapsulation.

While a number of natural and synthetic thermosensitive materials have been used for drug encapsulation [10], control of drug release in vivo remains a major challenge. Passive drug loading in hydrogels often results in rapid release due to the inability of many materials to retain lower molecular weight molecules [11]. While drug release kinetics can be delayed by further encapsulation within various microparticle systems, the resulting formulations are more complicated to synthesize and may not fully address burst release [12–14]. Covalent attachment of drugs offers greater control over long-term in vivo delivery, as release typically depends upon enzymatic or hydrolytic cleavage of the chemical bond between the drug and biomaterial [15]. Burst release can therefore be reduced [16,17], while appropriate temporal and spatial release profiles can be designed through environmentally responsive drug linkers [18].

Among the more commonly-used thermosensitive hydrogels are those based on poly(ethylene glycol) (PEG) [19,20], poly(N-isopropylacrylamide) (PNIPAM) [21], and hyaluronic acid blended with methylcellulose (HAMC) [22]. For cell encapsulation, materials such as chitosan [23] and collagen [24] have been used in addition to PEG [20], PNIPAM [21], and HAMC [25]. A chief requirement for these hydrogels is their biocompatibility for the particular cell type to be cultured and delivered in vivo. While modification of hydrogels with cell adhesion peptides or growth factors can affect cell attachment [26], proliferation [26], and differentiation [25], it is possible that incorporation of certain molecules could significantly alter the polymer LCST, thereby shifting a polymer's LCST outside of the temperature range useful for physiological applications [1,27].

Thus, there remains a need for tunable thermosensitive materials that can be readily conjugated to biologic drugs, while also serving as vehicles for delivery of cellular therapies. The Lutz group has pioneered the development of thermosensitive hydrogels synthesized by atom transfer radical polymerization (ATRP) of oligo(ethylene glycol) methyl ether methacrylate ($OEGMA_{475}$) and di(ethylene glycol) methyl ether methacrylate (MEO_2MA) from the arms of a 4-arm PEG ATRP macroinitiator [28,29]. These materials have the advantage of a tunable LCST that depends on the ratio of the two thermosensitive monomers. As a result, the monomer proportions can theoretically be adjusted to maintain an LCST near physiological temperature even in the presence of hydrophobic or hydrophilic drugs. Additionally, linear polymers composed mostly of the same monomers have been shown to be non-toxic at concentrations up to 10 mg/mL [30]. Despite these attractive characteristics, controllable drug conjugation is not possible due to the lack of functional groups in these materials.

The goal of this work was therefore (i) to synthesize injectable hydrogels incorporating functional monomers for facile drug conjugation and (ii) to characterize the physical and toxicological properties of the resulting biomaterials. Polymers containing MEO_2MA, $OEGMA_{475}$, and amine-reactive methacrylic acid N-hydroxysuccinimide ester (NHSMA) or amine-containing 2-aminoethyl methacrylate (AEMA) monomers were synthesized. Moreover, activators regenerated by electron transfer (ARGET) ATRP [31,32] was used rather than traditional ATRP because this approach requires less cytotoxic copper catalyst and is insensitive to small amounts of oxygen, allowing for reaction monitoring by NMR. A model peptide, bivalirudin, was then conjugated to the NHSMA-containing polymer; this material was used to demonstrate that polymer thermosensitivity can be iteratively tuned to compensate for changes in hydrophilicity due to conjugation of a peptide. Finally, a study of cellular biocompatibility for potential cell encapsulation applications revealed significant cytotoxicity to cultured mammalian fibroblasts and T-cells. The mechanism of this toxicity was tested, with data suggesting high polymer concentration and release of toxic degradation products as contributing factors, thus precluding the use of these materials for cell encapsulation and delivery. The results suggested, however, that the polymers may retain potential utility as localized drug delivery depots.

2. Experimental section

2.1. Materials and methods

Materials were purchased from Sigma-Aldrich unless otherwise noted.

2.1.1. Macroinitiator synthesis

A 4-arm PEG macroinitiator similar to that reported previously was synthesized [28]. In a typical reaction, 1 g (0.1 mmol) of 4-arm amine-terminated PEG, (MW 10,000, Laysan Bio) was dissolved in 10 mL anhydrous dichloromethane (DCM). The solution was placed under argon and cooled in an ice water bath over a stir plate. 223 μL of triethylamine (1.6 mmol) was subsequently added, and following a 10 minute wait, 202 μL (1.6 mmol) of α-bromoisobutyryl bromide was added. The reaction was stirred for 30 min before removing the vessel from the ice water and allowing it to reach room temperature. The solution was stirred overnight at room temperature. A separatory funnel with 4 mL of aqueous sodium chloride solution (~3.6 g/mL) was used to purify the reaction mixture. The organic phase was collected and dried for several hours with anhydrous magnesium sulfate. The product was then precipitated in ether and dried under vacuum and characterized by NMR. Yields were typically 0.5–0.7 g.

2.1.2. Synthesis of sPEG-b-P(MEO_2MA-co-$OEGMA_{475}$-co-NHSMA) by ARGET ATRP

In a typical reaction, 175.6 mg (0.018 mmol) of 4-arm PEG macroinitiator was added to a 10 mL round bottom flask and dissolved in 5 mL anhydrous anisole. 183.4 μL (0.417 mmol) of $OEGMA_{475}$, 1.944 mL (10.01 mmol) of MEO_2MA, and 97.4 mg (0.521 mmol) of NHSMA (TCI America) were subsequently added. The desired amounts of $CuBr_2$ (0.180 μmol, 0.04 mg) and tris(2-pyridylmethyl)amine (TPMA) (0.9 μmol, 0.267 mg) were so small as to make weighing difficult, so a stock suspension was prepared. 1 mg $CuBr_2$ and 6.6 mg TPMA were added to 1 mL anisole in a 1.5 mL microcentrifuge tube. The suspension was sonicated, vortexed, and vigorously pipetted to evenly disperse the insoluble $CuBr_2$. During rapid pipetting, 40 μL (~0.04 mg $CuBr_2$, 0.267 mg TPMA) was taken from the suspension and added to the 10 mL flask containing the monomers and initiator. A stir bar was added to the flask before it was sealed with a rubber septum and purged with argon for approximately 5 min. 3.1 μL (0.009 mmol) of $Sn(EH)_2$ was dissolved in 1 mL anisole and added to the purged reaction mixture via syringe. The flask was added to an oil bath preheated to 40 °C and the reaction was stirred for 2–3 days. Samples were periodically withdrawn via syringe and analyzed by NMR to determine polymer conversion. When conversion approached 50–60%, the reaction was stopped by removing it from the oil bath and removing the septum. The polymer was precipitated in approximately 140 mL diethyl ether, redissolved in acetone, and transferred into dialysis tubing (Spectropore, #132660, MW cutoff 6–8 kDa). The polymer was dialyzed against acetone for 1–2 days before being concentrated with a rotary evaporator.

2.1.3. Synthesis of sPEG-b-P(MEO_2MA-co-$OEGMA_{475}$-co-AEMA) by ARGET ATRP

In a typical reaction, 175.6 mg (0.018 mmol) of 4-arm PEG macroinitiator was added to a 10 mL round bottom flask and dissolved in 5 mL anhydrous anisole. 183.4 μL (0.417 mmol) of $OEGMA_{475}$, 1.944 mL (10.01 mmol) of MEO_2MA, and 87.8 mg (0.527 mmol) of AEMA were subsequently added, along with 2.5 mL of 100% ethanol to facilitate dissolution of AEMA. The desired amounts of $CuBr_2$ (0.18 μmol, 0.04 mg) and TPMA (0.9 μmol, 0.267 mg) were added via the same method as described for NHSMA hydrogels. A stir bar was added to the flask before it was sealed with a rubber septum and purged with argon for 5–10 min. 4.6 μL (0.0135 mmol) of $Sn(EH)_2$ was dissolved in 1 mL anisole and added to the purged reaction mixture via syringe. The flask was added to an oil bath preheated to 40 °C and the reaction was stirred for 2–3 days. Samples were periodically withdrawn via syringe and analyzed by NMR to determine polymer conversion. When conversion approached approximately 60%, the reaction was stopped by removing it from the oil bath and removing the septum. The polymer was precipitated in approximately 140 mL diethyl ether, redissolved in water, and transferred into dialysis tubing (Thermo Scientific #68100, MW cutoff 10 kDa). The polymer was dialyzed against water for 1–2 days before being concentrated with a rotary evaporator.

2.1.4. Peptide conjugation

To demonstrate functionalization of the hydrogel with a therapeutically relevant molecule, bivalirudin peptide was conjugated via its N-terminal amine to hydrogels containing NHSMA [33]. 30 mg of polymer was dissolved in 500 μL DMSO, while 23 mg peptide was dissolved separately in another 500 μL DMSO. The solutions were combined in a 1.5 mL microcentrifuge tube, followed by addition of 20 μL triethylamine and a small stir bar. The tube was suspended in an oil bath at 50 °C and stirred overnight. Following the reaction, the conjugate was dialyzed against water and eventually lyophilized. Peptide concentration and conjugation efficiency were determined from 280 nm absorbance measured on a Nanodrop 200c spectrophotometer (Thermo Scientific).

2.2. Measurement and analysis

2.2.1. ^1H NMR

^1H NMR spectra were recorded on a 500 MHz Bruker instrument using $CDCl_3$ as the solvent.

2.2.2. Gel permeation chromatography

GPC instrumentation consisted of Tosoh SEC TSK-GEL α-3000 and α-4000 columns connected in series to an Agilent 1200 Series Liquid Chromatography System, along with a Wyatt Technology miniDAWN TREOS, 3 angle MALS light scattering instrument and Optilab T-rEX, refractive index detector. A mobile phase of dimethylformamide containing 0.1% w/v LiBr was used with a flow rate of 1 mL/min at 60 °C. 30 kDa polystyrene standards were used for GPC calibration.

2.2.3. Cloudpoints

Polymer cloudpoints in phosphate buffered saline were measured using an Agilent 8453 UV–vis Spectrophotometer. Absorbance of a dilute polymer solution (3–10 mg/mL) in a standard 1 cm cuvette was measured at a wavelength of 670 nm. The temperature was raised slowly in increments of 1 °C with a 1 min hold at each temperature prior to the absorbance reading. The LCST was calculated as the temperature at which the absorbance reached a midpoint between the baseline and first plateau reading.

2.2.4. Tube inversion

For visual inspection of gelation, hydrogel solutions were immersed in warm water at various temperatures before subsequent removal and inversion. The extent to which the hydrogel flowed or remained stationary under gravity was observed.

2.2.5. Rheometry

An AR-G2 rheometer (TA Instruments) equipped with a Peltier plate temperature system was used to quantitatively describe the hydrogel change in viscosity with increasing temperature. Unconjugated hydrogels were tested using a 40 mm steel cone geometry with a 2° angle. The temperature was raised in 1° increments, with a 45 s hold prior to each measurement. At each temperature, a constant stress of 0.1 Pa was maintained while an angular frequency of 1 rad/s was applied. Storage and loss moduli were measured, and viscosity was calculated from the ratio of the loss modulus to the angular frequency.

Rheometry tests on the peptide-polymer conjugate were performed on an Anton-Paar instrument using a 25 mm cone with a 2° angle. Testing parameters were the same as above.

2.2.6. ICP-MS measurement of copper concentration

To quantify the amount of copper catalyst remaining in the polymer after dialysis, ICP-MS analysis was conducted on a PerkinElmer ELAN DRC-e instrument.

2.2.7. H9 cell culture

Human H9 CD4 + T cells were cultured in RPMI 1640 + 10% heat-inactivated FBS and passaged 1:5 in T25 flasks every other day, maintaining a density of $2–3 \times 10^5$ cells/mL.

2.2.8. NIH/3T3 cell culture

NIH/3T3 fibroblasts (ATCC) were cultured according to the supplier's instructions. Cells were cultured in DMEM + 10% FBS and passaged every 3 days with 3×10^5 cells in a T25 flask.

2.2.9. H9 cytotoxicity assays

For polymer cytotoxicity assays, polymers were first weighed out and dissolved in media overnight at 4 °C for a final concentration of 180 mg/mL polymer. H9 cells were then suspended in 100 μL polymer solution at a density of 3×10^5 cells/mL, plated in a 96-well plate, and incubated, at which point the polymer solution transitioned from a liquid to a gel state. For other treatments, cells were treated with OEGMA (12 mM), MEO_2MA (820 mM), linear polymers (4 mM), and macroinitiator (1 mM) dissolved in cell media at polymer-equivalent doses. For Transwell studies, cells were either placed in direct contact with gel ("Contact") or loaded in a Transwell support ("Transwell", Corning 0.4 μm) above gel. For DEGME and PEG cytotoxicity studies, DEGME (TCI America) and PEG (Sigma) were dissolved in cell media and diluted accordingly prior to treatment. For copper cytotoxicity studies, copper standard solution (Sigma) was diluted to polymer-relevant concentrations in cell media prior to treatment. All treatments were performed in triplicate.

2.2.10. NIH/3T3 encapsulation studies

NIH/3T3 cells (1×10^4) were resuspended in 100 μL cell media or polymer pre-dissolved in cell media (90 or 180 mg/mL) and seeded in a 96 well plate. Cells were allowed to grow for 24 h, and the wells were washed twice with 150 μL cell media and collected. Wells were then washed with 150 μL PBS, collected, and trypsin (30 μL) was added briefly to collect any attached cells. Cell media (150 μL) was then added to each well and then collected. Cell suspensions was then centrifuged (150 RCF for 5 min), resuspended in 150 μL PI buffer (PBS + 1% BSA + 2 μg/mL propidium iodide), and then analyzed by flow cytometry using 140 μL.

2.2.11. NIH/3T3 Transwell studies

NIH/3T3 cells were initially grown for 3 days prior to treatment. In a 24 well plate, 600 μL cell media was added to each treatment well, and Transwell inserts were placed. The plate and inserts were allowed to incubate for 1 h in a cell incubator. After, 5×10^3 cells/100 μL cell media was added to each insert, and cells were allowed to grow for 3 days. The following treatments were prepared on day 3 in a fresh 24 well

plate: unstained and untreated: 600 μL cell media in well; Transwell only: 600 μL cell media in well; polymer only: 200 μL of 180 mg/mL polymer pre-dissolved in media; polymer-treated: 200 μL of 180 mg/mL polymer pre-dissolved in media. The treatment plate was allowed to incubate in a cell incubator for 30 min after which 400 μL of pre-warmed media was added to each polymer only and polymer-treated well. Transwell inserts were then transferred from their original plate to the treatment plate after replacing the cell media in the insert and allowed to incubate for 48 h. After, the media was replaced with PBS, 30 μL trypsin was added to each insert, and each insert was washed twice with 150 μL of cell media. The cell suspension was centrifuged and resuspended in 100 μL PI buffer and analyzed by flow cytometry using 90 μL.

2.2.12. Flow cytometry

For flow cytometry analysis, cells were washed with PBS and centrifuged (300 RCF, 5 min, 4 °C). The supernatant was removed to isolate cells, and the cells were washed with PBS again. Cells were then suspended in PBS + 0.2% BSA + 2 μg/mL propidium iodide, and analyzed by flow cytometry (Miltenyi MACSQuant). Gating was set with the appropriate unstained and untreated controls.

2.2.13. Hemolysis assay

Red blood cells (RBCs) were isolated from donor blood as we have described previously [34]. Briefly, after centrifugation and washing with 150 mM NaCl, RBCs were treated with polymer dissolved in 100 mM phosphate buffer at various concentrations (45, 90, and 180 mg/mL). RBCs were then incubated for 1 h at 37 °C, and the supernatant was assessed using a plate reader (Tecan Safire2) at 541 nm. Treatments were performed in triplicate.

3. Results and discussion

In this work, amine-reactive sPEG-b-P(MEO_2MA-*co*-$OEGMA_{475}$-*co*-NHSMA) and amine-functionalized sPEG-b-P(MEO_2MA-*co*-$OEGMA_{475}$-*co*-AEMA) thermosensitive polymers were synthesized by ARGET ATRP using a 4-arm PEG macroinitiator (Fig. 1).

Successful synthesis of a 4-arm PEG macroinitiator was confirmed by ^1H NMR (Fig. S1). To determine the reaction efficiency of the four PEG arms, the integrated peak at 2 ppm corresponding to the terminal methyl hydrogens was compared with the peak at 3.6 ppm corresponding to the ethylene oxide hydrogens. A ratio greater than 0.025 was considered indicative of a sufficiently complete decoration based on a theoretical calculation of the number of methyl hydrogens relative to ethylene oxide hydrogens in the 10 kDa molecule. The described reaction using an amine-terminated 4-arm PEG represents an alternative macroinitiator synthesis method relative to the previously described synthesis using hydroxy-terminated PEG [28].

Initial attempts to synthesize 4-arm polymers by standard ATRP resulted in polymers with very large molecular weights and high polydispersity index (PDI > 3). The change to the ARGET ATRP technique led to synthesis of well-defined polymers. The ARGET method allowed for sampling of the reaction mixture in order to monitor monomer conversion and avoid excessively large molecular weights. In addition, the monomer concentration and catalyst levels were optimized to achieve a slower and better controlled reaction relative to standard ATRP. A

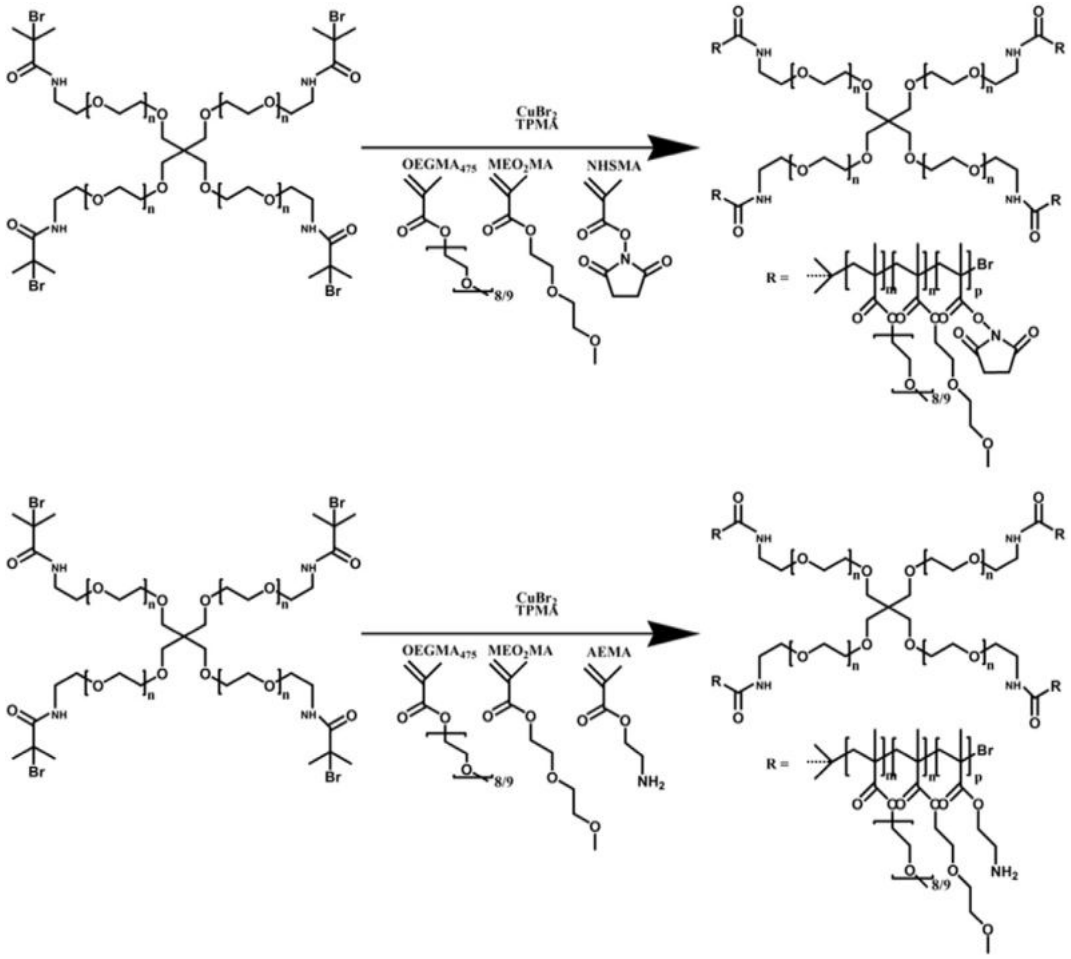

Fig. 1. Reaction schematics for ARGET ATRP synthesis of functionalized sPEG-*b*-P(MEO_2MA-*co*-$OEGMA_{475}$-*co*-NHSMA) and sPEG-*b*-P(MEO_2MA-*co*-$OEGMA_{475}$-*co*-AEMA).

monomer concentration of approximately 1.3 M was found to improve reaction control for sPEG-*b*-P(MEO_2MA-*co*-$OEGMA_{475}$-*co*-NHSMA) polymers relative to the starting concentration of approximately 2 M. Similarly, a monomer concentration of approximately 1 M allowed for synthesis of well-defined sPEG-*b*-P(MEO_2MA-*co*-$OEGMA_{475}$-*co*-AEMA) polymers. With very dilute reactions and low catalyst levels for the sPEG-*b*-P(MEO_2MA-*co*-$OEGMA_{475}$-*co*-AEMA), a 50% increase in the amount of reducing agent was employed to avoid excessively slow reaction rates.

The amine-reactive copolymer was initially synthesized by polymerization of the thermosensitive MEO_2MA and OEGMA monomers at a molar ratio of 96:4, with addition of 5% NHSMA. The resulting polymer was found by GPC to have M_w = 232 kDa and PDI = 1.3. Incorporation of NHSMA was verified on NMR by observation of a small peak at approximately 2.8 ppm (Fig. 2A). NHSMA content was estimated from NMR by using the integrated signals at 4.1 ppm (2 hydrogen atoms adjacent to $OEGMA_{475}$ and MEO_2MA ester bonds) and 2.8 ppm (4 NHS ester hydrogens) to determine the ratio of NHSMA to $OEGMA_{475}$ and MEO_2MA. Polymers were determined to contain approximately 7% NHSMA (5% feed amount), indicating that the NHSMA monomer is slightly more reactive than the $OEGMA_{475}$ and MEO_2MA monomers.

The polymer gelation behavior was qualitatively assessed by a tube inversion test, demonstrating formation of a free-standing hydrogel after brief (<60 s) incubation at 37 °C (Fig. 2B). Polymer concentrations between 15 and 20% w/v (150–200 mg/mL) in phosphate buffered saline (PBS) were typically required for gelation. Polymer gelation and the effect of the NHSMA monomer were quantitatively assessed by rheometry testing, which showed an expected increase in viscosity with increasing temperature (Fig. 2C). Relative to unmodified polymers, polymers incorporating the NHSMA monomer (~5%) had a lower gelation temperature by approximately 5 °C. The gelation temperature

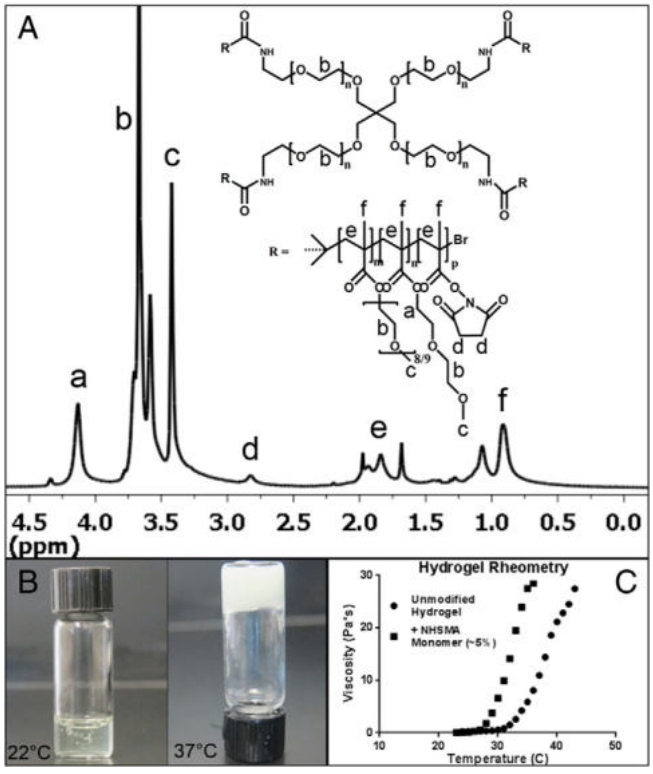

Fig. 2. A) NMR spectrum of sPEG-*b*-P(MEO_2MA-*co*-$OEGMA_{475}$-*co*-NHSMA). B) Tube inversion test illustrating that the polymer forms a free-standing gel at physiological temperature (37 °C). C) Rheometry testing demonstrating an increase in polymer viscosity with temperature, along with a leftward curve shift (decreased gelation temperature) for polymers incorporating NHSMA.

could be raised by increasing the $OEGMA_{475}$ proportion relative to the more hydrophobic MEO_2MA monomer.

Next, amine-functionalized polymers were synthesized by copolymerization of the thermosensitive MEO_2MA and OEGMA monomers at a molar ratio of 96:4, with addition of 5% AEMA. The resulting polymers were also relatively well-defined, with M_w = 336 kDa and PDI = 1.5. Incorporation of the hydrophilic AEMA monomer was evident by a significant increase in polymer LCST relative to unmodified polymers. As with the sPEG-*b*-P(MEO_2MA-*co*-$OEGMA_{475}$-*co*-NHSMA) polymers, the LCST of the polymer could be restored to physiologic temperature by changing the relative proportions of the thermosensitive monomers. Interestingly, while a dilute solution of sPEG-*b*-P(MEO_2MA-*co*-$OEGMA_{475}$-*co*-AEMA) polymer had a cloud point near 37 °C, rheometry testing of a concentrated solution showed gelation at a much higher temperature of approximately 55 °C (Fig. 3B). The lack of correlation between the cloud point and gelation temperature of the AEMA polymer is likely related to the hydrophilic nature of the monomer. A recent analysis of the phase transition of linear MEO_2MA-*co*-$OEGMA_{475}$ polymers describes the phenomenon beginning with collapse of the oxyethylene side chains towards the hydrophobic backbone [35]. The dehydrated polymer chains then loosely aggregate into physically cross-linked micelles as the LCST is approached. As the temperature increases above the LCST, the micelles aggregate more densely as water continues to be expelled from the vicinity of the polymer chains. The initial collapse of MEO_2MA and $OEGMA_{475}$ moieties should occur in the same manner for the 4-arm AEMA polymers, but the hydrophilic primary amine of the AEMA moiety likely limits the overall dehydration of the polymer chain. As a result, the hydrophobic interactions driving micelle formation would be weaker relative to a corresponding polymer without AEMA. It would therefore be expected that a temperature considerably higher than the LCST may be required to achieve the dense micelle aggregation necessary for hydrogel formation. This effect can likely be compensated for by further increasing the proportion of the more hydrophobic MEO_2MA monomer.

Next, we conjugated a model peptide drug, bivalirudin, to sPEG-*b*-P(MEO_2MA-*co*-$OEGMA_{475}$-*co*-NHSMA) to test conjugation efficiency and to assess the effect of peptide grafting on polymer properties. Successful conjugation of peptide to the polymer was confirmed by an increase in absorbance at 280 nm (Fig. 4A). Using the absorbance and an extinction coefficient of 1280 M^{-1} cm^{-1}, the conjugation efficiency for a representative sample was estimated to be 31.3%, corresponding to approximately 12 peptides/polymer. A leftward GPC shift was also observed after conjugation, consistent with an increase in molecular weight due to the peptide (Fig. 4C). Conjugation of the peptide to polymer with a 94:6 ratio of MEO_2MA to $OEGMA_{475}$ resulted in polymers with improved solubility, but also an associated increase in the LCST far above physiological temperature. Whereas unconjugated polymers had an LCST near 29 °C, the addition of the bivalirudin peptide increased the LCST to approximately 53 °C. In order to compensate for the hydrophilicity of the peptide, conjugation was repeated with polymers containing a higher molar ratio of MEO_2MA to $OEGMA_{475}$ (98:2 or 100:0). The subsequent peptide–polymer conjugates had lower LCSTs which were at or below physiological temperature (Fig. 4B). The peptide–polymer conjugate with a 98:2 ratio of MEO_2MA to $OEGMA_{475}$ had an LCST near 35 °C, which would be appropriate for in vivo applications as an injectable hydrogel. This ability to tune the polymer LCST in response to the solubility of the desired drug to be incorporated greatly enhances the potential utility of the material for delivery of a variety of therapeutic molecules.

The 98:2 polymer–peptide conjugate was observed to undergo gelation upon heating to physiological temperature, but higher concentrations (~30% w/v) were required relative to the unconjugated polymer. The increased concentration was likely needed as a result of the bivalirudin peptide inhibiting dense micelle aggregation near the LCST. This could be due in part to the peptide being relatively hydrophilic, but also may involve a steric effect from having multiple peptides

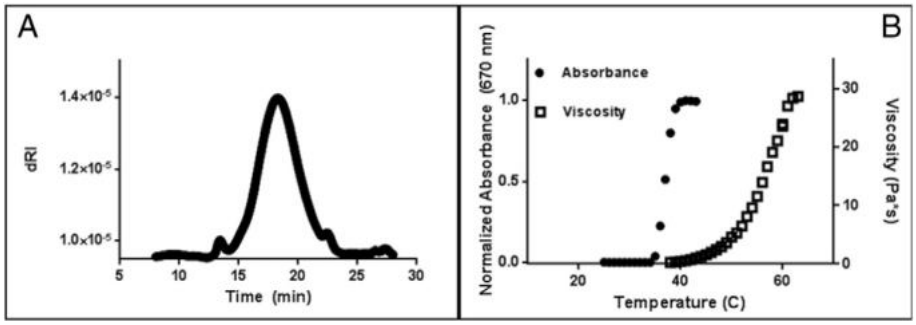

Fig. 3. A) Gel permeation chromatography trace of sPEG-*b*-P(MEO_2MA-*co*-$OEGMA_{475}$-*co*-AEMA). M_w = 336 kDa, PDI = 1.5. B) Absorbance (670 nm) and rheometry thermosensitivity measurements for sPEG-*b*-P(MEO_2MA-*co*-$OEGMA_{475}$-*co*-AEMA) polymers. While the cloud point of a dilute solution was near physiological temperature, gelation temperature of a concentrated solution was considerably higher (~55 °C).

attached to each polymer chain. Although the rheometry measurement showed a decrease in viscosity between approximately 20 and 35 °C (Fig. 4D), tube inversion revealed a free-standing gel following incubation at 37 °C. This apparent contradiction may be due to syneresis during gelation, in which case the rheometry measurement may reflect properties of both the gel and water that has been expelled. Of importance for practical application is the fact that the polymer is injectable in a cooled state, and readily forms a hydrogel as it warms to physiological temperature. Additional iterations of the material can further alter the peptide load and thermosensitive gelation characteristics.

Here we have developed a well-defined, synthetic polymer that can be used as an injectable hydrogel carrying a therapeutically relevant peptide for potential treatment of spinal cord injury. A potential bioactive peptide, bivalirudin, was directly conjugated to the polymer as a proof of concept for covalent attachment, and also to demonstrate how polymer thermosensitivity may be tuned to compensate for hydrophilicity of an incorporated therapeutic molecule. While this method is not necessarily expected to achieve desired drug release kinetics, future work may include the development of a controlled release system in which the peptide is covalently attached to the polymer through an environmentally-responsive, degradable linker. For example, the use of matrix metalloproteinase substrate linkers to attach therapeutic peptides may allow for temporally regulated drug release in the SCI environment [7].

The base polymer containing MEO_2MA and $OEGMA_{475}$ at a ratio of 96:4 was also tested as a carrier for cell therapy applications. To test the cell compatibility of the polymer, human H9 T-cells were cultured in solutions at various polymer concentrations (45, 90, and 180 mg/mL) and evaluated at several time points (30 min, 60 min, 24 h, 48 h) by flow cytometry for cell viability. Human H9 cells are CD4+ and

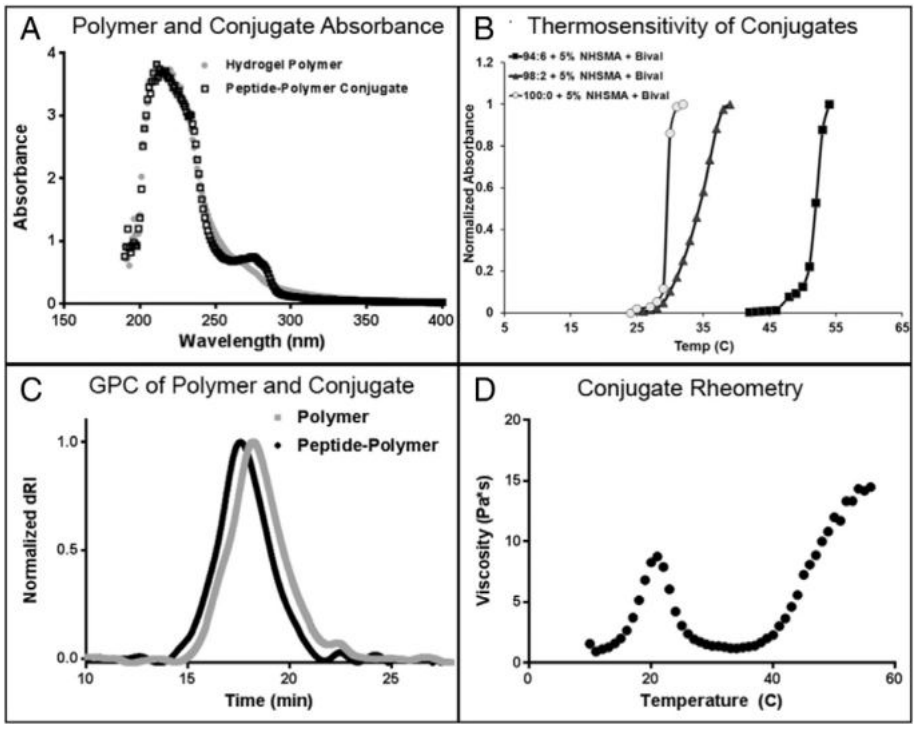

Fig. 4. A) Absorbance spectrum of the peptide–polymer conjugate, showing an increase at 280 nm relative to polymer without peptide. B) Absorbance (670 nm) measurements for peptide–polymer conjugates with varying proportions of MEO_2MA and $OEGMA_{475}$. The LCST can be tuned using the ratio of thermosensitive monomers to compensate for the hydrophilic peptide. C) GPC traces of sPEG-*b*-P(MEO_2MA-*co*-$OEGMA_{475}$-*co*-NHSMA) polymer before and after peptide conjugation. The conjugate shows a leftward shift, consistent with an increase in molecular weight from the peptide. D) Rheometry of peptide–polymer conjugate, showing distinct phases in which the viscosity rises, falls (likely due to syneresis), and rises again with increasing temperature. A tube inversion test at 37 °C demonstrated a free standing gel.

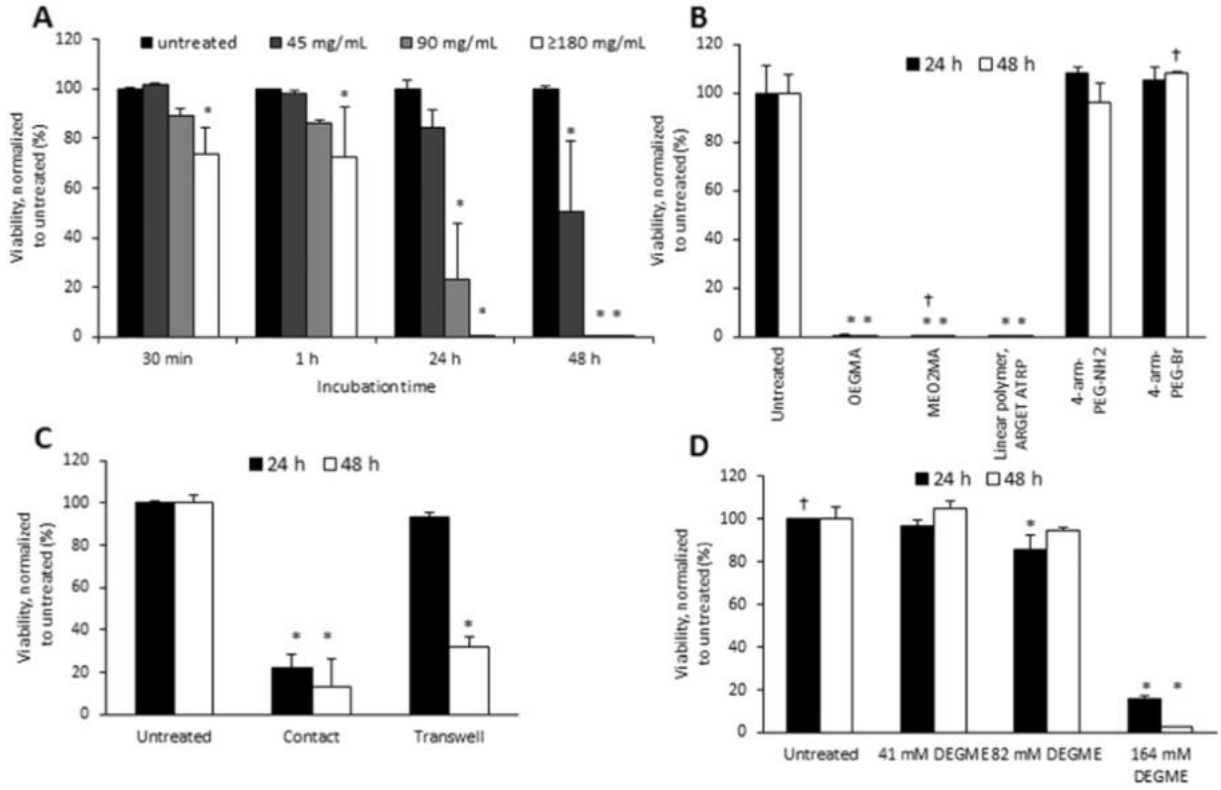

Fig. 5. A) Viability over time of cells encapsulated in various polymer concentrations. B) Viability of cells treated with polymer-equivalent concentrations of monomers, linear polymer, macroinitiator precursor, and macroinitiator. C) Viability of cells deposited directly on gel ("Contact") or separated from gel by a Transwell insert ("Transwell"). D) Viability of cells treated with 41 mM, 82 mM, and 164 mM of DEGME, modeling 5%, 10%, and 20% MEO_2MA hydrolysis, respectively. Treatments performed in triplicate, except when †n = 2. Data reported are the mean ± standard deviation. Statistical analysis was performed with a two-way ANOVA followed by a post hoc Dunnett's multiple comparisons test. *p-value < 0.05.

have been used extensively as a model of primary T-cells [36–38]. Culture in the presence of the polymer was found to be highly cytotoxic, with significant cell death observed at the earliest time point (30 min) for concentrations above 45 mg/mL (Fig. 5A). At the 180 mg/mL concentration, encapsulation within the hydrogel led to complete cell death by 24 h. While the hydrogels originally reported by Lutz et al. have been described as biocompatible [29], the materials reported in that work were not examined at the high concentrations necessary for gelation and cell encapsulation.

To better understand the origin of cytotoxicity, cells were cultured in the presence of the following polymer components: individual monomers, the 4-arm PEG macroinitiator, amine-terminated 4-arm PEG, and linear polymers synthesized from a small molecule initiator. While the 4-arm PEG molecules were not cytotoxic at the relevant concentrations, the linear polymers and individual monomers killed virtually all cells by 24 h (Fig. 5B). To determine whether degradation products of the hydrogel may contribute to the observed cytotoxicity, cells were incubated directly on top of hydrogels (rather than encapsulated), or separated from the hydrogel by a Transwell insert. While the Transwell insert seemed to improve cell viability compared to direct gel contact, significant cytotoxicity was still observed at 48 h post-treatment (Fig. 5C). This result suggests that a degradation product was leaching from the polymer, or that some proportion of the polymer at the hydrogel surface was released into the culture medium. Given that the ester bond present within the MEO_2MA monomer is subject to hydrolysis, we hypothesized that release of the diethylene glycol monomethyl ether (DEGME) hydrolysis product may contribute to cytotoxicity. To test this, we evaluated the cytotoxicity of three concentrations (41, 82, and 164 mM) of DEGME, which modeled 5%, 10%, and 20% hydrolysis of the MEO_2MA monomer, respectively. DEGME exhibited concentration-dependent cytotoxicity (Fig. 5D), with significant cytotoxicity observed at 164 mM DEGME (modeling 20% MEO_2MA hydrolysis) for both 24 and 48 h incubations. While the extent of hydrolysis in the hydrogel cell culture experiments could not be accurately quantified, our data establishes release of DEGME as a potential contributing factor to the observed cytotoxicity.

The possibility that the amphiphilic polymer might cause membrane lysis was examined through a hemolysis assay using human red blood cells (Fig. 6A). While the polymers did exhibit concentration-dependent cytotoxicity with 6.04 ± 3.38% hemolysis at the highest tested concentration (180 mg/mL), this level is negligible compared to highly membrane-lytic polymers, which have exhibited up to 70% hemolysis with concentrations as low as 40 μg/mL [39]. Cell membrane disruption is therefore unlikely to be a major cause of cytotoxicity with these polymers.

As the polymers in this work were synthesized by ARGET ATRP, components of the synthesis process, specifically the copper(II) bromide catalyst [40] and the tin(II) 2-ethylhexanoate reducing agent, could potentially induce cell death. Cell culture experiments demonstrated that while copper levels of 5 and 25 ng/mL appeared to induce cytotoxicity at 24 h, some degree of recovery was apparent at 48 h (Fig. 6B). ICP-MS analysis revealed that actual polymer copper levels were below 0.025 ng/mL, more than 200-fold less than the levels causing relatively minor cell death in culture. Therefore, copper does not appear to contribute significantly to hydrogel cytotoxicity. To determine effects of tin, linear polymers were synthesized by standard ATRP, which does not use a reducing agent. Polymers made by standard and ARGET ATRP were equally cytotoxic, suggesting that tin is unlikely to be a factor (Fig. 6C).

A relatively high polymer concentration is required to achieve gelation for cell encapsulation. We next determined the extent to which cytotoxicity may be dependent on polymer concentration, rather than some property of the particular molecular structure. H9 cells were cultured in poly(ethylene glycol) (PEG) polymers of various molecular

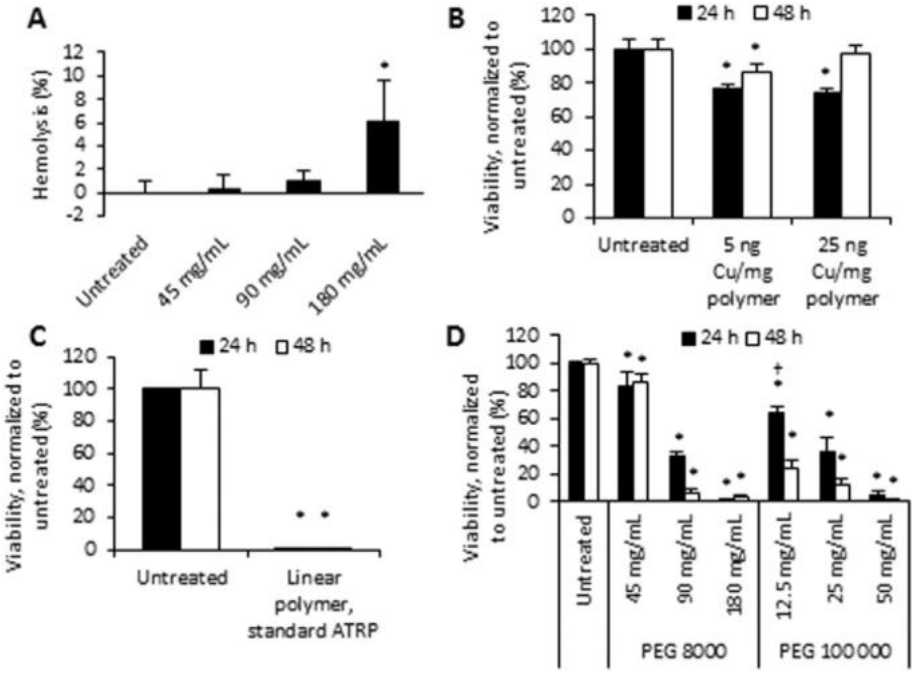

Fig. 6. A) Hemolysis of red blood cells treated with various concentrations of polymer, compared to 100% by Triton X-100 hemolysis. B) Viability of cells treated with polymer-relevant concentrations of copper. C) Viability of cells treated with linear polymers synthesized via standard ATRP at a polymer-equivalent concentration. D) Viability of cells treated with increasing concentrations of PEG 8000 and PEG 100,000. Treatments performed in triplicate, except when †n = 2. Data reported are the mean ± standard deviation. Statistical analysis was performed with a two-way ANOVA followed by a post hoc Dunnett's multiple comparisons test (A, B, D) or a post hoc Sidak's multiple comparisons test (C). *p-value < 0.05.

weight (8000 and 100,000) dissolved in media at various concentrations for comparison with the hydrogel polymers. Although PEG is considered a highly biocompatible polymer, cytotoxicity was observed even at concentrations far below 180 mg/mL (Fig. 6D).

To assess whether the observed cytotoxicity may vary with cell type, NIH/3T3 fibroblasts were also examined in two culture conditions. Cells were either encapsulated in polymer solutions of varying concentration (90 mg/mL, 180 mg/mL), or separated from the hydrogel (180 mg/mL) by a Transwell insert. Encapsulation was found to be highly cytotoxic (>90% cell death) after 24 h at both concentrations, similar to H9 cells (Fig. 7a). The Transwell condition, however, did not result in significant cytotoxicity for NIH/3T3 cells, with average viability maintained above 90% after 48 h (Fig. 7b). Thus, the IC_{50} of hydrolysis products or other material released from the hydrogel is likely dependent on cell type. This supports the potential use of the polymer as a CNS drug-delivery depot, as surrounding tissue would be exposed to low levels of degradation products rather than being encapsulated in the hydrogel. In addition, it would be expected that such material would undergo some clearance due to cerebrospinal fluid circulation, limiting potential accumulation.

While the materials reported here appear suitable for controlled drug delivery applications, reduced gelation concentrations are needed in the next generation OEGMA-based materials for cell encapsulation. One potential approach to reduce polymer concentration is to combine a biocompatible natural material with the synthetic polymer, as has been done previously with PEG and chitosan [8,41]. Modifying the structure or architecture of the synthetic polymer could also potentially change the gelation behavior [42]. Block copolymers in which relatively hydrophilic blocks surround a relatively hydrophobic block have been suggested to form micelles that lead to gelation with increased

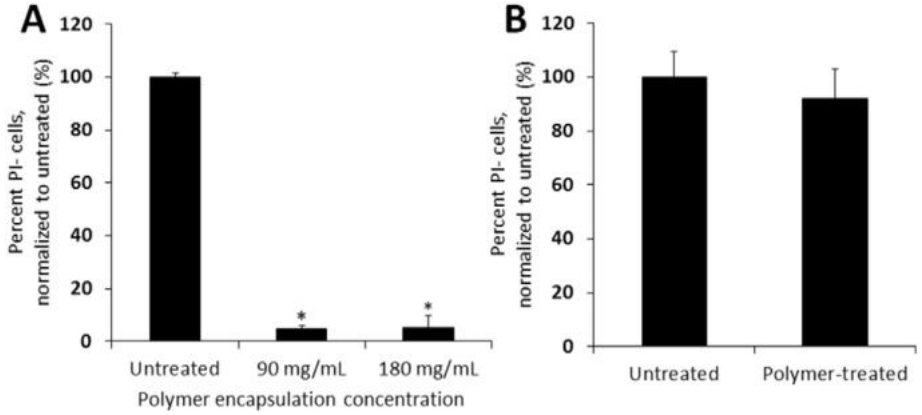

Fig. 7. A) Percent propidium iodide (PI) negative NIH/3T3 cells 24 h after encapsulation in various polymer concentrations. Treatments performed in triplicate. Data reported are the mean ± standard deviation. B) Percent PI-NIH/3T3 cells 48 h after physical separation from hydrogel by a Transwell insert ("Polymer-treated"), normalized to untreated. Statistical analysis was performed with a one-way ANOVA followed by a post hoc Dunnett's multiple comparisons test (A), or a two-tailed Student's *t*-test (B). *p-value < 0.05 compared to untreated.

temperature [19]. Block copolymers might therefore allow for gelation at a lower concentration, relative to the random copolymers synthesized in this work. Similarly, the use of a more highly branched polymer (e.g., 8-arm) could conceivably strengthen hydrophobic interactions above the LCST, leading to gelation at a reduced concentration.

4. Conclusions

This work has demonstrated the synthesis and characterization of an injectable hydrogel biomaterial with tunable thermosensitivity and the capability for covalent attachment of therapeutic peptides. The ratio of thermosensitive monomers can be varied to compensate for the incorporation of a relatively hydrophilic drug, thereby maintaining an appropriate gelation temperature for physiological applications. Although the required polymer concentration of the present formulation is not suitable for cell encapsulation, the hydrogel has potential utility for controlled drug delivery in soft tissue applications.

Supplementary data to this article can be found online at http://dx.doi.org/10.1016/j.jconrel.2015.03.003.

Author contributions

The manuscript was written through contributions of all authors. All authors have given approval to the final version of the manuscript.

Funding sources

This work was supported by a CDMRP SCRIP Investigator Initiated Award (SC130249), a postdoctoral fellowship from the Craig H. Neilsen Foundation (259216) (PZE), and a National Science Foundation Graduate Research Fellowship (2013163401) (GWL).

Abbreviations

$OEGMA_{475}$	oligo(ethylene glycol) methyl ether methacrylate, molecular weight 475
MEO_2MA	di(ethylene glycol) methyl ether methacrylate
NHSMA	methacrylic acid N-hydroxysuccinimide ester
AEMA	2-aminoethyl methacrylate
ATRP	atom transfer radical polymerization
LCST	lower critical solution temperature

References

[1] B. Jeong, S.W. Kim, Y.H. Bae, Thermosensitive sol–gel reversible hydrogels, Adv. Drug Deliv. Rev. 54 (1) (2002) 37–51.
[2] L. Yu, J. Ding, Injectable hydrogels as unique biomedical materials, Chem. Soc. Rev. 37 (2008) 1473–1481.
[3] D.J. Begley, Delivery of therapeutic agents to the central nervous system: the problems and the possibilities, Pharmacol. Ther. 104 (1) (2004) 29–45.
[4] M.M. Pakulska, B.G. Ballios, M.S. Shoichet, Injectable hydrogels for central nervous system therapy, Biomed. Mater. 7 (2) (2012) 024101.
[5] F. Rossi, G. Perale, S. Papa, G. Forloni, P. Veglianese, Current options for drug delivery to the spinal cord, Expert Opin. Drug Deliv. 10 (3) (2013) 385–396.
[6] D. Fisher, B. Xing, J. Dill, H. Li, H.H. Hoang, Z. Zhao, X.L. Yang, R. Bachoo, S. Cannon, F.M. Longo, M. Sheng, J. Silver, S. Li, Leukocyte common antigen-related phosphatase is a functional receptor for chondroitin sulfate proteoglycan axon growth inhibitors, J. Neurosci. 31 (40) (2011) 14051–14066.
[7] D.S. Chu, D.L. Sellers, M.J. Bocek, A.E. Fischedick, P.J. Horner, MMP9-sensitive polymers mediate environmentally-responsive bivalirudin release and thrombin inhibition, Biomater. Sci. 3 (2015) 41–45.
[8] C. Tsao, F. Kievit, A. Ravanpay, A. Erickson, M. Jensen, R. Ellenbogen, M. Zhang, Thermoreversible poly(ethylen glycol)-g-chitosan hydrogel as a therapeutic T lymphocyte depot for localized glioblastoma immunotherapy, Biomacromolecules 15 (7) (2014) 2656–2662.
[9] Z. Zou, E. Denny, C.E. Brown, M.C. Jensen, G. Li, T. Fujii, J. Neman, R. Jandial, M. Chen, Cytotoxic T lymphocyte trafficking and survival in an augmented fibrin matrix carrier, PLoS One 7 (4) (2012) e34652.
[10] J.D. Kretlow, L. Klouda, A.G. Mikos, Injectable matrices and scaffolds for drug delivery in tissue engineering, Adv. Drug Deliv. Rev. 59 (4–5) (2007) 263–273.
[11] X. Huang, C.S. Brazel, On the importance and mechanisms of burst release in matrix-controlled drug delivery systems, J. Control. Release 73 (2–3) (2001) 121–136.
[12] S.D. Allison, Analysis of initial burst in PLGA microparticles, Expert Opin. Drug Deliv. 5 (6) (2008) 615–628.
[13] Y. Yeo, K. Park, Control of encapsulation efficiency and initial burst in polymeric microparticle systems, Arch. Pharm. Res. 27 (1) (2004) 1–12.
[14] D.L. Sellers, T.H. Kim, C.W. Mount, S.H. Pun, P.J. Horner, Poly(lactic-co-glycolic) acid microspheres encapsulated in pluronic F-127 prolong hirudin delivery and improve functional recovery from a demyelination lesion, Biomaterials 35 (31) (2014) 8895–8902.
[15] T. Hoare, D. Kohane, Hydrogels in drug delivery: progress and challenges, Polymer 49 (2008) 1993–2007.
[16] Y. Suzuki, M. Tanihara, K. Suzuki, A. Saitou, W. Sufan, Y. Nishimura, Alginate hydrogel linked with synthetic oligopeptide derived from BMP-2 allows ectopic osteoinduction in vivo, J. Biomed. Mater. Res. 50 (3) (2000) 405–409.
[17] V. Luginbuehl, L. Meinel, H.P. Merkle, B. Gander, Localized delivery of growth factors for bone repair, Eur. J. Pharm. Biopharm. 58 (2) (2004) 197–208.
[18] J.A. Burdick, W.L. Murphy, Moving from static to dynamic complexity in hydrogel design, Nat. Commun. 3 (2012) 1269.
[19] B. Jeong, Y.H. Bae, S.W. Kim, Drug release from biodegradable injectable thermosensitive hydrogel of PEG-PLGA-PEG triblock copolymers, J. Control. Release 63 (1–2) (2000) 155–163.
[20] J.A. Burdick, K.S. Anseth, Photoencapsulation of osteoblasts in injectable RGD-modified PEG hydrogels for bone tissue engineering, Biomaterials 23 (22) (2002) 4315–4323.
[21] L. Conova, J. Vernengo, Y. Jin, B.T. Himes, B. Neuhuber, I. Fischer, A. Lowman, J. Vernengo, Y. Jin, B.T. Himes, B. Neuhuber, I. Fischer, A. Lowman, A pilot study of poly(N-isopropylacrylamide)-g-polyethylene glycol and poly(N-isopropylacrylamide)-g-methylcellulose branched copolymers as injectable scaffolds for local delivery of neurotrophins and cellular transplants into the injured spinal cord, J. Neurosurg. Spine 15 (6) (2011) 594–604.
[22] M.D. Baumann, C.E. Kang, J.C. Stanwick, Y. Wang, H. Kim, Y. Lapitsky, M.S. Shoichet, An injectable drug delivery platform for sustained combination therapy, J. Control. Release 138 (3) (2009) 205–213.
[23] K.E. Crompton, J.D. Goud, R.V. Bellamkonda, T.R. Gengenbach, D.I. Finkelstein, M.K. Horne, J.S. Forsythe, Polylysine-functionalised thermoresponsive chitosan hydrogel for neural tissue engineering, Biomaterials 28 (3) (2007) 441–449.
[24] D. Macaya, K. Ng, M. Spector, Injectable collagen–genipin gel for the treatment of spinal cord injury: in vitro studies, Adv. Funct. Mater. 21 (24) (2011) 4788–4797.
[25] R. Tam, M. Cook, M. Shoichet, A covalently modified hydrogel blend of hyaluronan–methyl cellulose with peptides and growth factors influences neural stem/progenitor cell fate, J. Mater. Chem. 22 (2012) 19402–19411.
[26] X.Z. Shu, K. Ghosh, Y. Liu, F.S. Palumbo, Y. Luo, R.A. Clark, G.D. Prestwich, Attachment and spreading of fibroblasts on an RGD peptide-modified injectable hyaluronan hydrogel, J. Biomed. Mater. Res. A 68 (2) (2004) 365–375.
[27] R. Yoshida, K. Sakai, T. Okano, Y. Sakurai, Modulating the phase transition temperature and thermosensitivity in N-isopropylacrylamide copolymer gels, J. Biomater. Sci. Polym. Ed. 6 (6) (1994) 585–598.
[28] N. Fechler, N. Badi, K. Schade, S. Pfeifer, J.-F. Lutz, Thermogelation of PEG-based macromolecules of controlled architecture, Macromolecules 42 (1) (2008) 33–36.
[29] N. Badi, J.F. Lutz, PEG-based thermogels: applicability in physiological media, J. Control. Release 140 (3) (2009) 224–229.
[30] J. Lutz, J. Andrieu, S. Uzgun, C. Rudolph, S. Agarwal, Biocompatible, thermoresponsive, and biodegradable: simple preparation of "all-in-one" biorelevant polymers, Macromolecules 40 (2007) 8540–8543.
[31] K. Matyjaszewski, Atom Transfer Radical Polymerization (ATRP): current status and future perspectives, Macromolecules 45 (2012) 4015–4039.
[32] S. Yamamoto, K. Matyjaszewski, ARGET ATRP synthesis of thermally responsive polymers with oligo(ethylene oxide) units, Polym. J. 40 (6) (2008) 496–497.
[33] M.J. Yanjarappa, K.V. Gujraty, A. Joshi, A. Saraph, R.S. Kane, Synthesis of copolymers containing an active ester of methacrylic acid by RAFT: controlled molecular weight scaffolds for biofunctionalization, Biomacromolecules 7 (5) (2006) 1665–1670.
[34] J.G. Schellinger, J.A. Pahang, J. Shi, S.H. Pun, Block copolymers containing a hydrophobic domain of membrane-lytic peptides form micellar structures and are effective gene delivery agents, ACS Macro Lett. 2 (8) (2013) 725–730.
[35] S. Sun, P. Wu, On the thermally reversible dynamic hydration behavior of oligo(ethylene glycol) methacrylate-based polymers in water, Macromolecules 46 (2013) 236–246.
[36] R.L. Rowell, D. Fairhurst, S. Key, A. Morfesis, I.M. Monahan, M. Mitchnick, R.A. Shattock, Microbicides for HIV/AIDS. 1. Electrophoretic fingerprinting the H9 cell model system, Langmuir 21 (22) (2005) 10165–10171.
[37] T.R. Chen, Karyotypic derivation of H9 cell line expressing human immunodeficiency virus susceptibility, J. Natl. Cancer Inst. 84 (24) (1992) 1922–1926.
[38] D.L. Bolton, B.I. Hahn, E.A. Park, L.L. Lehnhoff, F. Hornung, M.J. Lenardo, Death of CD4(+) T-cell lines caused by human immunodeficiency virus type 1 does not depend on caspases or apoptosis, J. Virol. 76 (10) (2002) 5094–5107.
[39] J.G. Schelliner, J.A. Pahang, J. Shi, S.H. Pun, Block copolymers containing a hydrophobic domain of membrane-lytic peptides form micellar structures and are effective gene delivery agents, ACS Macro Lett. 2 (2013) 725–730.
[40] R.M. Broyer, G.N. Grover, H.D. Maynard, Emerging synthetic approaches for protein–polymer conjugations, Chem. Commun. (Camb.) (2011) 2212–2226.
[41] N. Bhattarai, H.R. Ramay, J. Gunn, F.A. Matsen, M. Zhang, PEG-grafted chitosan as an injectable thermosensitive hydrogel for sustained protein release, J. Control. Release 103 (3) (2005) 609–624.
[42] H.-H. Lin, Y.-L. Cheng, In-situ thermoreversible gelation of block and star copolymers of poly(ethylene glycol) and poly(n-isopropylacrylamide) of varying architectures, Macromolecules 34 (2001) 3710–3715.